JOURNAL OF MATERIALS SCIENCE **34** (1999) 5387–5395

Generation of novel microstructures in rapidly foamed polybutylene terephthalate

KWANGJIN SONG, WENGUANG LI*, JAMES O. ECKERT JR.‡, DAVID WU, ROBERT E. APFEL**
Department of Mechanical Engineering, Yale University, New Haven, CT 06520-8286;
‡*Department of Geology and Geophysics, Yale University, New Haven, CT 06520-8286*
E-mail: kwangjin.song@yale.edu

A novel technology called "Dynamic Decompression and Cooling (DDC) Process" for producing foams from semicrystalline polymers has been developed. In the present experiment, a solution of polybutylene terephthalate (PBT) melt and blowing liquid ($CHCl_3$) is processed under high pressure and temperature. As the system is decompressed above the boiling point of the solvent, phase separation occurs; gas bubbles nucleate out from a metastable regime and grow through evaporation of the volatile phase and diffusion of non-condensable gas. Solidification is achieved by crystallization of the polymer and supercooling of the melt induced by the latent heat of vaporization of the volatile phase. The resulting foams have open, interconnected cell structures with densities of 10–20% of the original materials. Structural characterization with DSC, SEM and X-ray diffraction techniques reveals that the DDC foams are semicrystalline with crystallinity of ca. 35% and possess a variety of micromorphologies as well as crystalline orientations. This structural character is believed to modify considerably the mechanical properties of the fabricated DDC foams.

1. Introduction

Polymeric foams have been commercially used for decades [1, 2]. The foams may be produced by dispersing a gas into the liquid phase or by generating a gas in the liquid phase. The mechanism of this foam formation generally involves the pressure difference between the inside of the cell and the surrounding medium [3]. The pressure difference may be created either by decompressing the system or by increasing the internal cell pressure. Foams can be also generated by leaching of a fugitive phase from a polymer or sintering of small particles under heat and pressure. The foams fabricated may possess open or closed cell structures depending on processes and materials. The state of the art in the production of polymeric foams has been recently advanced in many respects.

Extrusion and injection molding processes are widely used for producing thermoplastic foams of polystyrene and polyethylene [1–3]. Polymers with physical/chemical blowing agents are blended in an extruder, where plastification and mixing take place under high temperature and pressure. The bubbles nucleate by a gradient in temperature or pressure. The extrudates expand and are stabilized into foams either by cooling or chemical reactions. The method of thermally induced liquid-liquid phase separation to produce filled microporous polymers was first described in a 1981 patent by Castro [4]. A two-phase heterogeneous solution is obtained by rapid quenching of homogeneous polymer solutions into the demixing region. Subsequent removal of the solvent phase leaves polymer foams with a void structure on a micrometer scale [5–8]. Patents by Suh *et al.* [9–12] at MIT in the 1980s proposed a different microcellular foaming technology, in which a polymer is saturated with a high pressure gas such as nitrogen or carbon dioxide. The solution is then depressurized and/or cooled into foams. Goel and Beckman [13] in the early 1990s described a "constant-temperature variable-pressure" process for generating microcellular polymeric foams using supercritical carbon dioxide. An amorphous polymer is saturated with CO_2 at high pressures of 25–35 MPa for a sufficiently long time. A rapid pressure quench from this equilibrium state leads to the formation of polymers with void structures. Another new approach for producing cellular solids, which is called "Dynamic Decompression and Cooling (DDC) Process," has been introduced in a 1995 patent by Apfel [14]. This technology involves heating and mixing of materials under pressure in the presence of a volatile phase. A rapid decompression of the mixture induces the volatile phase to evaporate causing the melt to cool rapidly and expand.

* *Current address*: 550 Research Parkway, Meriden, CT 06540.
** Author to whom all correspondence should be addressed.

A previous experiment using the DDC process [15, 16] showed that an organic p-terphenyl/water mixture was processed into foams with an open cell structure and a density as low as 12% of the original material. The cooling rate achieved by DDC reached at least 100 °C/s. It is our purpose in this work to produce foams from thermoplastic polymers using the DDC technology. We first apply this technique to a polymer, polybutylene terephthalate (PBT), which tends to crystallize rapidly. We will describe processing characteristics as well as structure evolution of PBT in the DDC foaming process. The resulting DDC foams are structurally characterized. Special attention is given to the characterization of microstructures in the foams.

2. Experimental

2.1. Materials

The polymer used in this experiment was a polybutylene terephthalate (PBT) purchased from Aldrich Chemical Co. It had a molecular weight (M_v) of 38,000, an intrinsic viscosity (IV) of 0.66 dl/g, and a density of 1.310 g/cm^3. An HPLC-grade chloroform ($CHCl_3$) with 99.9% purity was used as a blowing liquid. Chloroform has a density of 1.482 g/cm^3 at 25 °C, a boiling point of 61.1 °C, a critical temperature of 236.2 °C and a critical pressure of 5.47 MPa. A mixture of 5 g PBT and 10 ml. $CHCl_3$ was used for each test throughout the experiments.

2.2. Sample preparation

The DDC process was designed and built in our laboratory using a modified PARR pressure cell (Fig. 1) [15]. It consists of three major parts: a stainless-steel pressure cell, a mixing unit and temperature/pressure controlling systems. A 50 ml glass beaker containing a mixture of PBT/$CHCl_3$ was placed inside the pressure vessel and then pressurized with N_2. The samples were heated up, while stirring, to a temperature of ca. 220 °C, around the crystalline melting point of PBT. After the polymers were completely melted, the heater was first turned off, followed about one minute later by the stirrer. The system cooled down naturally to a prescribed decompression temperature, where the release valve was quickly opened manually and the system was rapidly decompressed. For comparison, we prepared a blown film using a Killon tubular film extruder equipped with an annular die. The films were produced from a PBT of IV = 1.24 dl/g with blow-up ratio (BR) of 2 and a draw-down ratio (DR) of 40.

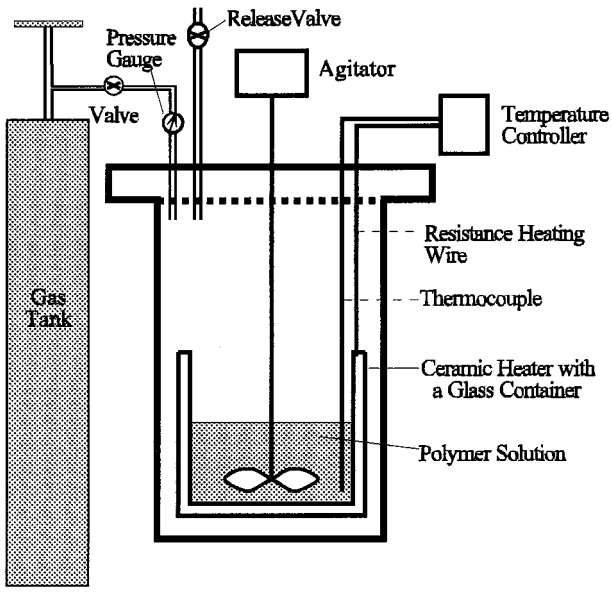

Figure 1 A schematic diagram of the DDC apparatus.

2.3. Characterization

Thermal analyses were performed over the temperature range from 0 to 250 °C with a Perkin-Elma Pyris-1 differential scanning calorimeter (DSC). The heating rate was 20 °C/min and the sample weight was 10.0 ± 0.2 mg. The instrument was calibrated using pure indium metal. The crystallinity of PBT samples was computed through:

$$X_c(\%) = \frac{\Delta H_{exp}}{\Delta H^o} \times 100 \qquad (1)$$

where $\Delta H_{exp} = \Delta H_{melting} - \Delta H_{cold\ crystallization}$, ΔH^o = 142 J/g given by Iller [17] as the heat of fusion of 100% crystalline PBT.

Morphologies of the foams produced were observed with a JEOL JXA-8600 electron microprobe, functioning as a scanning electron microscope (SEM). Fresh surfaces of the samples were prepared either by freeze-cutting or freeze-fracturing using liquid nitrogen. The surfaces were coated with a thin layer of carbon material to prevent charging by the electron beam.

Wide angle X-ray diffraction (WAXS) patterns were taken with Scintag and GE X-ray generators. The GE X-ray beam was monochromatized with a nickel foil filter to obtain CuK_α radiation. The foams were carefully cut into three parts from the bottom to top direction having dimensions of $20 \times 20 \times 3$ mm along the flow direction. Bragg angle scanning was then conducted for the three specimens over the 2θ range from 5 to 60°. In texture measurements, the $(0\,1\,0)\alpha$ and $(1\,0\,0)\alpha$ planes for the middle part of the foam were pole figured around two Eulerian angles at intervals χ of 5° and ϕ of 10°, respectively. The PBT triclinic unit cell of Hall and Pass [18] was approximated as pseudo-orthorhombic [19]. In this unit cell, the *c*-axis is along the chain axis, the *a*-axis is parallel to the phenyl ring normal, and the *b*-axis is taken orthogonal to the '*ac*' plane. White-Spruiell biaxial crystalline orientation factors are then calculated through [20]:

$$f^B_{1,j} = 2\overline{\cos^2\phi_{1,j}} + \overline{\cos^2\phi_{2,j}} - 1 \qquad (2)$$

$$f^B_{2,j} = 2\overline{\cos^2\phi_{2,j}} + \overline{\cos^2\phi_{1,j}} - 1 \qquad (3)$$

where $\phi_{i,j}$ is the angle between the sample direction i (1: flow direction (FD), 2: hoop direction (HD)) and the crystallographic axis j.

3. Results

3.1. DDC process

Choice of a proper blowing liquid is important for the successful DDC process. The blowing liquid may have

a low boiling point and a negligible solubility for polymers below its boiling temperature, but should dissolve the polymer under high temperature and pressure. Boiling point of the liquid influences how rapidly the expanded polymer will solidify and stabilize the cell structure. A number of solvents have been reported for polyesters including PBT [21–24]. East and Girshab [24] have used a mixture of chloroform/hexane (10/5, 10/3) as a solvent to dissolve oligomers extracted from PBT specimens. Our experiments revealed that PBT was not substantially soluble in chloroform until it began to melt at temperatures above 190 °C under pressure. A mixture of chloroform/hexane was also found to be a solvent, but hexane alone did not dissolve PBT polymers even under such elevated temperature and pressure conditions. We have used chloroform as a solvent for processing of PBT throughout the experiments.

In order to obtain optimal processing conditions, the pressures were varied from 2.41 to 4.48 MPa and the decompression temperatures from 125 to 225 °C. It was observed that at a fixed pressure of 3.45 MPa, a decrease in decompression temperature tended to increase foam density and caused the formation of some fine particles in the foam produced. Increasing pressure at a given release temperature of 150 °C, however, introduced marginal changes in foam density. We produced PBT foams with a density, measured by a water displacement technique, as low as 10–20% of the original material at release temperatures of 150–160 °C under starting pressures of 2.76–4.14 MPa. The whole cycle of each process from heating to decompression took about 10 min. The DDC foams produced under a decompression temperature of ca. 150 °C and a pressure of ca. 3.45 MPa have been structurally characterized. These foams revealed a density of ca. 15% of the original material.

3.2. WAXS Bragg angle scan

A PBT specimen quenched rapidly in a liquid N_2 bath exhibits an amorphous background in WAXS diffraction patterns (Fig. 2). A specimen cooled slowly in air, however, shows distinct crystalline reflections of the PBT α-form crystals. Reflections occur at d spacings of 9.83, 5.14, 4.41 and 3.83 Å. These are equivalent to the PBT (0 0 1), (0 1 0), ($\bar{1}$ 1 1), and (1 0 0) planes of the α phase. The (1 0 0)α peak is the most intense among them. The distributions of diffracted intensities are independent of the scanned direction. It shows that a blown film with low levels of deformation is characteristically similar to the specimen cooled slowly. The film, however, possesses more intense crystalline reflections particularly with a strong (0 1 0) peak. Strikingly, a PBT foam produced in the DDC process exhibits anisotropy of crystalline texture. Equatorial scans contain quite strong (0 1 0)α and (1 0 0)α peaks, while in the meridional scans, the (0 1 0)α reflection diminishes and the (1 0 0)α peak substantially intensifies. Diffraction patterns changed little with the sample position. The β-reflections are not seen in any of the specimens investigated.

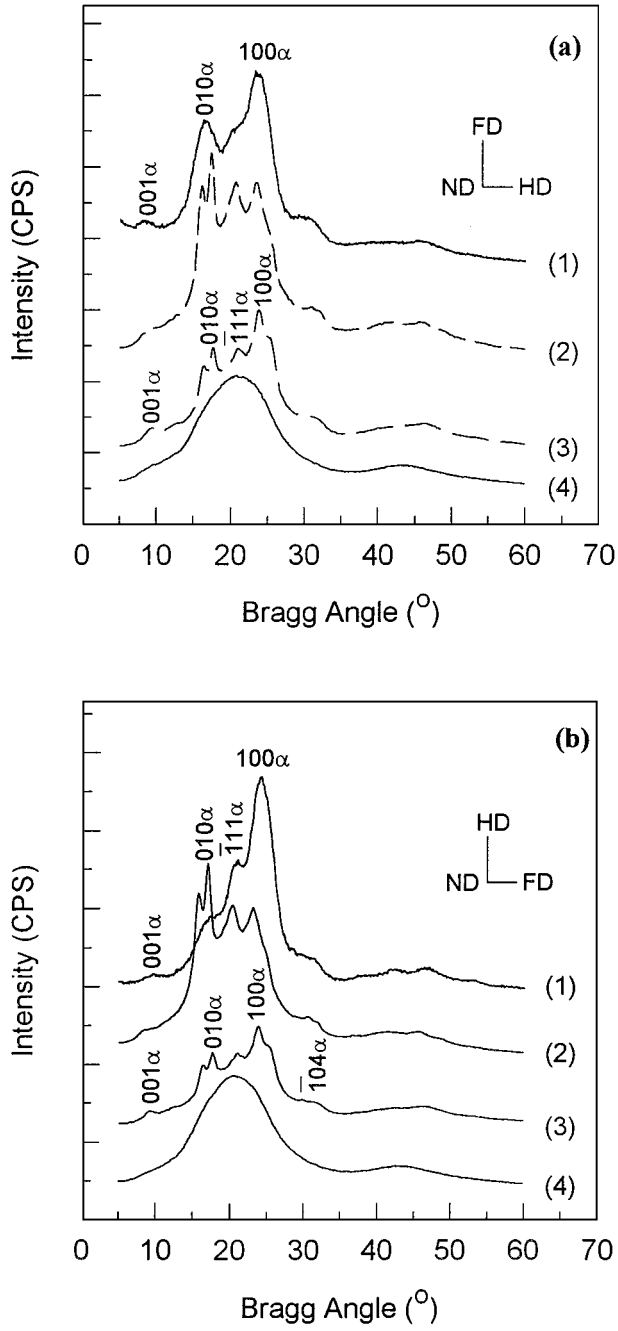

Figure 2 WAXS diffraction patterns of PBT samples produced under different conditions: (a) Equatorial scans: (1) DDC foam produced from 25 wt % PBT solutions in $CHCl_3$ at decompression temperature of 150 °C under 3.45 MPa, (2) Blown film with blowup ratio (BR) of 2 and drawdown ratio (DR) of 40, (3) PBT sample cooled slowly from the melt, (4) PBT sample quenched rapidly in a liquid nitrogen bath. (b) Meridional scans.

3.3. Differential scanning calorimeter

DSC thermograms of various PBT specimens are presented in Fig. 3. The rapidly cooled specimen displays a glass transition temperature (T_g) of 32 °C and a crystalline melting point (T_m) of 222 °C. The sample reveals a quite large melting endotherm. It is seen that both as-received PBT resin and a blown film with BR × DR = 2 × 40 are similar to the sample quenched rapidly. They have higher T_g's around 50 °C and T_m's around 224 °C. A DDC PBT foam is semicrystalline with a T_g of 45 °C and a T_m of 225 °C. The melting endotherm exhibits a shoulder at the higher

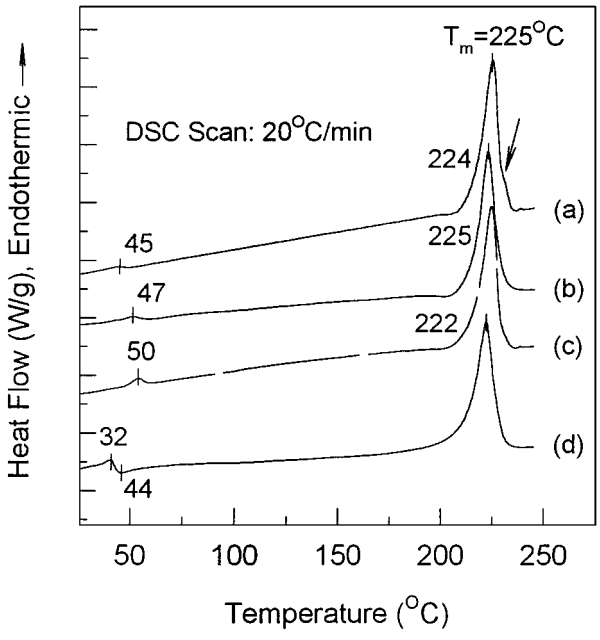

Figure 3 DSC thermograms of PBT polymers (a) DDC-produced PBT foam (b) Blown film with BR × DR = 2 × 40 (c) As-received resin (d) PBT sample quenched rapidly in a liquid nitrogen bath.

temperature region. No appreciable variations were observed in feature of DSC thermograms with the sample position.

3.4. Scanning electron microscope

DDC-produced PBT foams generally possess open cell structures with large distributions of pore size and shape (Fig. 4a). The sizes of elliptical cells vary from 10 to 1,000 μm in diameter. The cells are interconnected with each other. These features are similar to those of extruded open cell foams of low viscosity polymers. We have also observed the micromorphologies of the foams produced. A scanning electron micrograph, shown in Fig. 4b, exhibits a band of thin fibers with diameter as small as 100 nm. These microfibrils are aligned along the flow direction of the volatile phase occurring during decompression. This morphology is often seen in the upper part of the cylindrical foam. Fig. 4c shows morphology of granular aggregates with a diameter of several microns. There are pores as small as one micron in the aggregates. This morphology is frequently observed in the outer part of the sample. SEM images for the bottom part of the sample are shown in Fig. 4d and e. A sheet-like shape is seen in Fig. 4d. The sheets have a 10 μm thickness and become folded leaving a void structure similar to irregular channels. Fig. 4e contains a fiber web combined with some granules. This structure is quite unusual; it seems ideal to enhance the foam strength.

3.5. WAXS texture measurements

WAXS pole figures for the (0 1 0) and (1 0 0) planes of the PBT α-phase are presented in Fig. 5. A blown film deformed at blow-up ratio (BR) of 2 and draw-down ratio (DR) of 40 exhibited largely isotropic pole figures. The poles are randomly distributed in the plane of the film. The pole figures for a DDC PBT foam, however, comprise some concentrations of plane normals. The (1 0 0) poles concentrate in the normal direction (ND) with spreads toward the ND-HD plane. The poles with weak intensities are distributed along the flow direction of the volatile phase. It shows that the (0 1 0) poles spread in the HD-ND plane with higher intensities in the HD.

4. Discussion

4.1. Mechanism of DDC foam formation

In polymer-incompressible liquid solutions, the formation of void structure is largely associated with phase separation behavior of the binary system [5–8]. Phase separation can occur by fluctuations in temperature, pressure, and/or composition of the mixture [25], the mechanism of which depends on the state of thermodynamic stability of the system. When the system is in the metastable region, nucleation and growth predominate; while in the demixing region, spinodal decomposition is a likely mechanism of the phase transformation.

The initial state of the DDC process is a solution of polymer melt and solvent under high pressure nitrogen. As decompression is effected above the boiling point of the solvent, both supersaturation of non-condensable gas and superheating of the volatile phase occur. The system undergoes phase separation: bubbles nucleate and grow, controlled by evaporation of the volatile phase and diffusion of the non-condensable gas. Supercooling of the melt, which stabilizes the bubbles, occurs as the volatile phase takes its latent heat of vaporization from the melt. The degree and kind of crystallization of polymers involved in the foaming process depend on the decompression schedule and the cooling rate of the solution. PBT is a rapidly crystallizing polymer [26, 27]. This might help stabilize the bubbles through an increase in viscosity of the solution. In this experiment, a solution of PBT/$CHCl_3$ at ca. 220 °C under pressure was naturally cooled to the decompression temperature of 150 °C. Nichols *et al.* [28] reported that in a PBT/epoxy binary solution system (5–10 wt %), the crystallization of the PBT phase occurred around 180 °C, and liquid-liquid phase separation took place below 170 °C. The rate of crystallization increased with an increase of PBT content in solutions. A rapid quenching of the solution into the two-phase region, however, was found to induce phase separation followed by crystallization.

The mechanism of DDC foaming described above appears to be associated with a classical nucleation and growth process induced by rapid pressure quench. This generally agrees with that of solutions of polymers and blowing liquids in extrusion foaming processes [1–3, 21, 23]. Bubbles may nucleate out from a metastable regime during phase separation. This foaming mechanism suggests that the DDC technique can also produce open or closed-cell foams depending on material and process conditions. For moderately concentrated polymer solutions especially close to the critical concentrations, spinodal decomposition

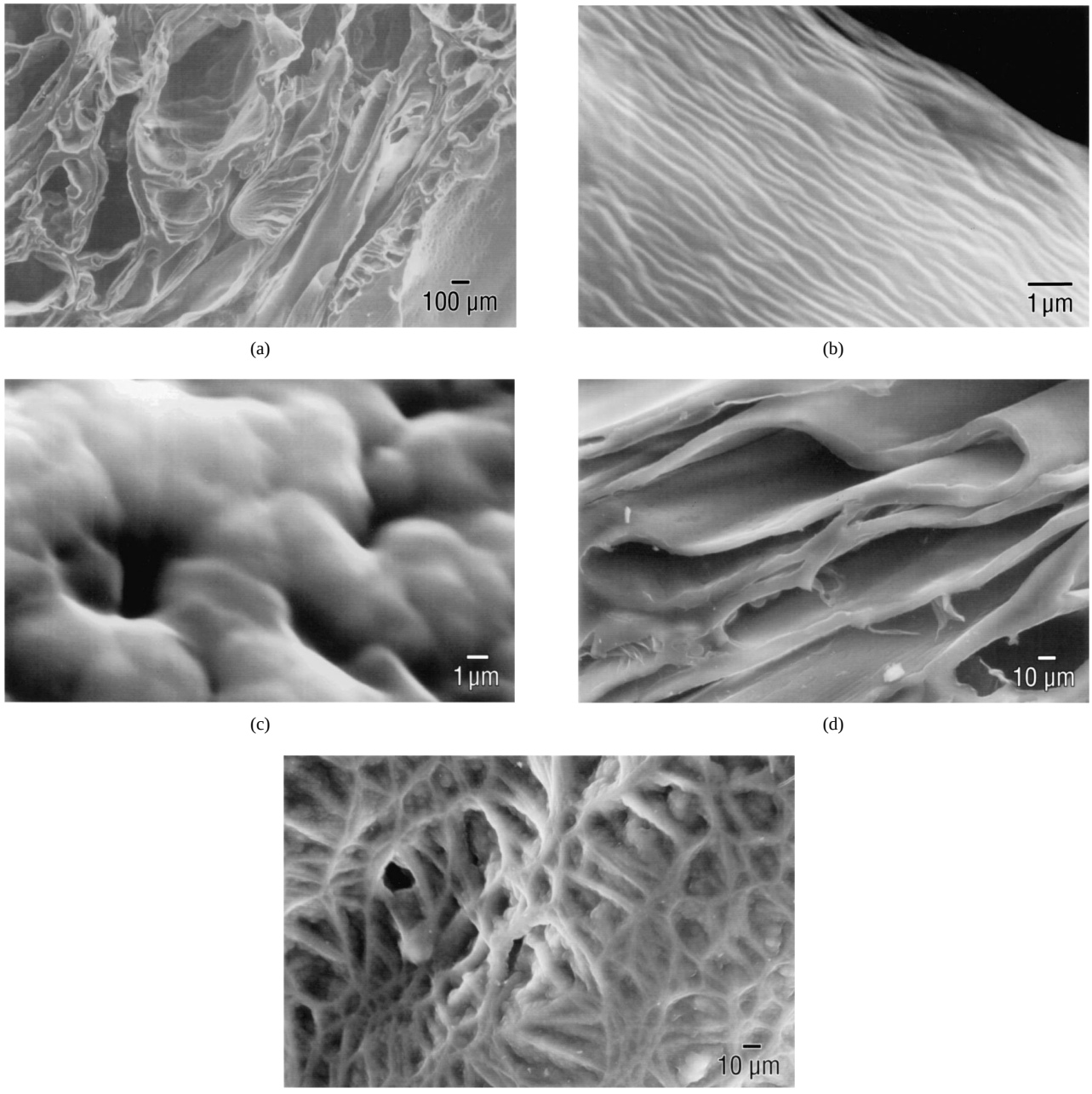

Figure 4 Scanning electron micrographs of DDC PBT foams produced from a solution of 25 wt% PBT/$CHCl_3$ decompressed at temperature of 150 °C and pressure of 3.45 MPa (see text) (a) SEM image taken from freeze-cut surface of the foams, (b), (c), (d), (e): SEM images taken from freeze-fractured surfaces of the foams.

is another possible mechanism of phase separation. This process, which is characterized by a highly interconnected bicontinuous phase, generates within an unstable mother phase a spontaneous and continuous growth of another phase [25]. Polymer solutions generally undergo spinodal decomposition when the system is rapidly cooled into the two-phase region. Foams produced from spinodally decomposed, relatively concentrated (10–20 wt%) polymer solutions, therefore, invariably possess open, interconnected cell structures due to phase interconnectivity [5–8]. Han and Han [29] claimed that in concentrated (40–60 wt%) polystyrene/toluene solutions, bubbles nucleated heterogeneously at the interface of the volatile liquid and another phase in contact with it. As the bubbles grew during the expansion process, they varied in size owing to heterogeneous nucleation as well as coalescence of nuclei. Lee and Shine [30] noted that in dilute polymer solutions, the polymer-rich phase induced by phase separation was dispersed as isolated droplets in the solvent sea. A rapid expansion, thus, of these supercritical solutions (RESS) resulted in micro-size polymer particles which contained no void structure [30–32].

Cellular structures of DDC foams can be related to material characteristics as well as processing variables such as level of pressure, decompression ratio, decompression temperature, and cooling rate. The material parameters are the most influential on this issue and may include mainly molecular weight, strain hardening behavior, and temperature-dependency of flow properties of polymers. In this experiment, we produced only open, interconnected void structures with large

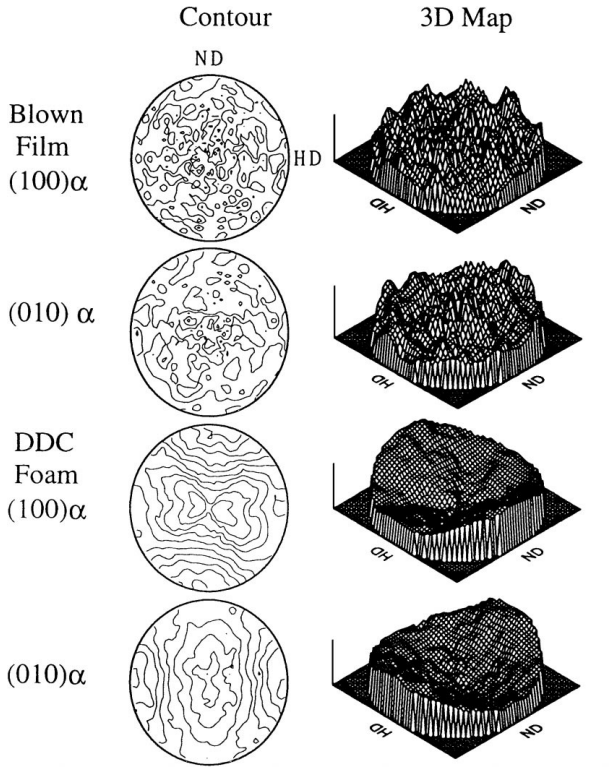

Figure 5 WAXS pole figures of the (1 0 0) and (0 1 0) plane of the PBT α-phase as a function of processing.

distributions in size and shape of cells. Changes in processing variables were found not to cause any structural transition from open to closed cells. It would seem that the open, interconnected cell structures of DDC foams are closely related to rupture of cell membranes during the expansion period rather than the mechanisms of phase separation. PBT has a lower melt viscosity than polyethylene terephthalate (PET) at comparable molecular weights [33]. This is due to a long flexible methylene segment of PBT molecule. During the decompression process, bubbles may experience heterogeneous nucleation and subsequent expansion almost explosive in nature, which as a result cause distributions of cell size and shape and fractal rupture of cell membranes. This behavior could be accounted for by low levels of melt strength, which stemmed from the low melt viscosity of the PBT processed. Generally, polymers with higher molecular weight produced more readily foams with a closed-cell structure [21, 23]. Khemani [34] reported that in extrusion foaming processes, a PET polymer with relatively high viscosity (IV = 0.7 dl/g) produced open cell structures unless crosslinking of the polymer was introduced. We have used a 25 wt % solution of PBT of relatively low molecular weight as a starting material.

4.2. Crystalline structure

A PBT sample quenched rapidly in liquid nitrogen exhibits distinct amorphous character in conventional WAXS $\theta/2\theta$ scans, while a sample cooled slowly is semicrystalline with the α-form crystal. No orientation is observed. The diffraction patterns are in good agreement with the triclinic unit cell of the PBT α-modification reported by Hall and Pass [18]. It is found that a blown film produced at low levels of deformation has more perfected crystals. Yet the texture is isotropic. A PBT foam produced by DDC possesses rather imperfect crystals with reflections overlapping. However, the crystallites in the foam have orientation, as suggested by the anisotropy of diffracted peaks. This crystalline character of the foam can be attributed to rapid cooling as well as extension of the material occurring during decompression. The absence of the β-phase indicates that the DDC foam underwent low or intermediate levels of extensional stresses. This can be ascribed in part to stretching of the polymer phase with no constraints at both ends. The extended chains may relax during stretch. A stable β-modification was observed in highly drawn fibers and films [35–37].

Several different values of T_g for PBT, which ranged from −25 to 60 °C determined from DSC, have been reported [26, 27, 38–41]. The T_g of ca. 28 °C is generally accepted for amorphous PBT [26, 27, 39, 40]. However, Chen *et al.* [38] and Avramova [41] reported a much lower T_g of −25 °C. During DSC scans, the DDC foam was found to crystallize more readily indicating the existence of chain orientation. Fig. 6 presents the crystallinities (X_c, %) of various PBT polymers. As-received PBT resin has an X_c of ca. 31%, which is higher than X_c = ca. 27% determined by density measurements. The crystallinity increases slightly with processing. A DDC PBT foam shows an X_c of ca. 35%. In contrast to the result of WAXS $\theta/2\theta$ scans, the sample quenched rapidly exhibits an X_c of ca. 24%. These are typical crystallization behavior of fast crystallizing polymers owing to the restructuring process during the DSC temperature scan. Multiple melting peaks have been found for PBT samples annealed from the glassy or melt state [42–46], which are usually interpreted in terms of preexisting morphology and/or reorganization during DSC scans [27, 42–47]. The appearance of double melting peaks in the DDC foam therefore suggests that the foam may have a larger distribution of crystal perfection. This structural variation in different PBT

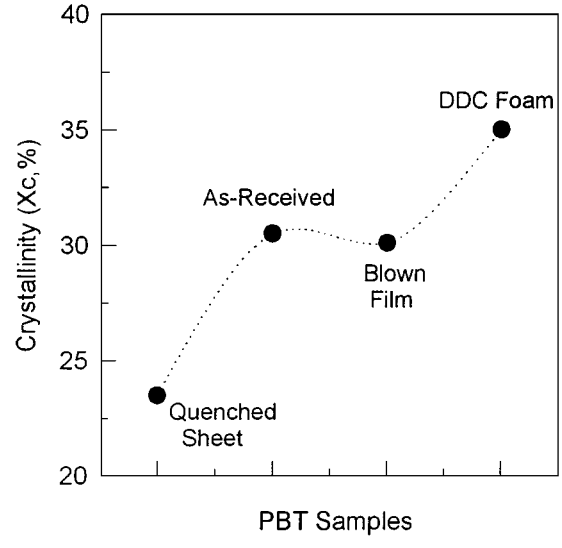

Figure 6 Crystallinities (X_c,%) of various PBT polymers determined from DSC measurements.

products may result from the differences in viscosity of the starting polymers and thermomechanical history that the materials experienced during processing.

4.3. Morphology of the DDC foam

Polymer foams are found to have some degrees of structural anisotropy in nature [48]. This anisotropy may arise from direction-dependent changes in the shape of the cells as well as the property of the cell wall itself. Our scanning electron micrographs of the DDC foams disclosed a variety of quite localized, atypical micromorphologies of fibers, granules, sheets and their mixtures, which reflect characteristics of solution grown crystals as well as flow-induced crystallization of the polymer in a confined space. In general, crystalline morphologies of polymers grown from solutions can vary substantially with a change in crystallization conditions such as temperature, solvent and concentration [49–51].

The initial state of the DDC process is non-isothermal: the system cools down naturally to the preset decompression temperature. Upon decompression, stress develops on the polymers at the cell walls, and the undercooling of the melt is likely to initiate at or near the bubble-liquid interface. The temperature, concentration and stress of the system may fluctuate locally and instantaneously due to the large irregularities in bubble size and shape. The flow of the solvent evaporation is preferentially unidirectional; thus, the polymers at the upper part of the container are exposed more heavily to the evaporating solvents and solidify more rapidly than those at the bottom part of the container. The polymer network, which retains some memory of mechanical stirring, experiences extension along the flow direction of the volatile phase. It would seem that this nonuniform nature of mass and heat flow as well as stress in DDC resulted in local fluctuations in both crystallizability and crystallization rate of the polymer, which in turn led to the formation of localized, diverse crystalline morphologies in the resultant foam. There may also exist temperature and stress gradients in the direction from the core to the skin of the foam. Radial expansion of bubbles is restricted by the glass container, which cools more slowly than the solution when decompression is effected. Crystalline morphologies of oriented fibrils, somewhat network-like lamellae, as well as spherulites are therefore generated. This crystalline character is consistent with the results of DSC and WAXS measurements. One may also expect a variety of flow-induced superstructures, which are localized and have originated from the uniqueness of the DDC process.

There have been extensive SEM studies on micromorphologies of polymeric materials [48–58]. Nichols *et al.* [28] observed polymer globules grown from PBT/epoxy solutions whose surfaces were rough and consisted of stacks of lamellae. Several authors reported well-defined spherulites grown from solution-cast PBT samples [27, 53, 55]. Wilkes and Chu [53] found that subsequent drawing of the solution-cast PBT samples caused the flattening of spherulites, giving rise to films with rough surfaces of flattened spherulites. These spherulites are characteristically similar to the granules found in our DDC foams (Figs 4c and e). Smith and Penning [54] also observed spherulitic structures from a free grown surface formed by solidification of eutectic solutions of polypropylene. Barham *et al.* [56] and Smith *et al.* [57] noted that in semidilute solutions of PE, mechanical stirring induced orientation of macromolecules, which in turn caused the formation of fiber network morphology consisting of shishkebab-like crystals. This morphology resembles the fiber web structure presented in Fig. 4e. Matson *et al.* [31, 32] and Lele and Shine [30] found that the micro-size precipitates of various polymers produced by RESS possessed various shape morphologies such as powders, fibers and films in scanning electron photomicrographs. They noted that the polymers, which had more time for phase separation, had a larger size and experienced larger elongation during RESS expansions resulting in the morphology of a fiber shape. Schaaf *et al.* [58] observed globules and multi-lamella assemblies grown from solutions of high density polyethylene. They argued that the formation of different morphologies from various polymer solutions was primarily governed by liquid-liquid phase separation followed by crystallization.

It appears that the micromorphologies described above by several authors are generally similar to those found in our DDC foams. However, the DDC foams exhibit a complicated, mixed feature of the individual micromorphologies. The development of morphology in DDC is clearly quite complex, whose mechanisms may involve such factors as liquid-liquid phase separation, concentration, heat and mass flows associated with the formation of void structure, shear-induced orientation of macromolecules and flow-induced deformation of the polymer phase. The SEM photomicrographs of DDC foams are therefore characterized as a solution-grown deformed structure, in which, at least in nature, cellular and crystalline morphologies mutually interact to produce some aspect of structural anisotropy. The DDC foams are found to differ considerably in morphology from those of conventional melt-extruded polymer foams [59]. This difference seems to arise primarily from the difference in processing of polymers. In the DDC process, semiconcentrated polymer solutions are formed into foams, while in extrusion processes, polymer melts plus physical/chemical blowing agents usually produce foams. The morphological character of DDC foams may provide a different class of applications for foams of thermoplastic polymers.

4.4. Crystalline orientation

In the triclinic unit cell of PBT α-foam crystal [18], the (0 1 0) plane makes an angle of 50.1° with the chain axis and 29.0° with the (1 0 0) plane. The (1 0 0) plane is roughly parallel to the plane of the phenyl ring on the chain backbone. The second moments of the orientation distribution have been determined by applying Wilchinsky's treatment [60]:

$$\overline{\cos^2 \phi_j} = \frac{\int_0^{2\pi} \int_0^{2\pi} I_{hkl}(\phi_1, \chi_1) \cos^2 \phi_1 \sin \phi_1 \, d\phi_1 \, d\chi_1}{\int_0^{2\pi} \int_0^{2\pi} I_{hkl}(\phi_1, \chi_1) \sin \phi_1 \, d\phi_1 \, d\chi_1} \quad (4)$$

where $I_{hkl}(\phi_1, \chi_1)$ is the diffracted intensity distribution in the pole figures. Using the directional cosine values of the (1 0 0) and (0 1 0) planes, one can obtain the following relationships for the *c*-axis (chain) and the *a*-axis (phenyl ring normal):

$$\overline{\cos^2\phi_{i,c}} = 1 - 1.14216\,\overline{\cos^2\phi_{i,100}} - 0.85874\,\overline{\cos^2\phi_{i,010}} \quad (5)$$

$$\overline{\cos^2\phi_{i,a}} = 1.16041\,\overline{\cos^2\phi_{i,100}} - 0.16041\,\overline{\cos^2\phi_{i,010}} \quad (6)$$

White-Spruiell biaxial crystalline orientation factors are then computed through Equations 2 and 3.

As might be expected, a blown film with BR × DR = 2 × 40 has $f^B_{i,j} \approx$ zero indicating little orientation of crystallites in the film. However, the DDC foam exhibits a considerable level of the chain orientation. The orientation factors for the *c*-axis have the values of $f^B_{c,FD} \approx 0.32$ (the flow direction) and $f^B_{c,HD} \approx 0.10$ (the hoop direction). The polymer chains are preferentially oriented along the flow direction. A rather weak hoop orientation may result from the geometric restriction of bubble expansion confined in a container. The *a*-axis has $f^B_{a,FD} \approx -0.25$ and $f^B_{a,HD} \approx -0.11$. The phenyl rings are aligned along the surface of the foam. The DDC PBT foam possesses (1 0 0) planar-axial orientation of the α-form crystals, where the levels of orientation are slightly lower than found in a film uniaxially stretched at $\lambda = 2$ [37]. Bonner *et al.* [23] made similar observations that foamed PET fibers produced from a solution of 50 wt% PET/CH_2Cl_2 extruded at 6.89 MPa through a small circular orifice had uniplanar orientation of crystallites: the *a*- and *b*-axes lie preferentially in the plane of the cell wall. It is believed that the development of orientation in the DDC process can modify considerably the mechanical properties of the foams produced.

5. Conclusions

We have reported here our initial work on application of "Dynamic Decompression and Cooling (DDC)" to foaming of thermoplastic polymers. DDC is found to be a very promising technology for producing lightweight, cellular materials of semicrystalline polymers. In DDC, polymer melt solutions under high pressure are processed into foams through pressure-induced phase separation. The foaming mechanism is considered a nucleation and growth process, which suggests the cellular structures of DDC foams can be modified by controlling material and process conditions. The polymer phase was found to undergo mild deformation during the expansion process. The resulting PBT foams are semicrystalline and possess open cell structures with a variety of flow-induced micromorphologies as well as crystalline orientation of the α phase. This structural character is a unique feature of the DDC technology, and the degree of structural anisotropy may possibly be controlled if some modifications are made on the apparatus. Although the technology appears to have great potential for producing foams of various thermoplastic polymers, it is in the very beginning stages of development. Our future studies will include the extension of DDC applications to other semicrystalline polymers, including blends, as well as the development of a theoretical model to improve our understanding of transient foaming mechanisms in DDC.

Acknowledgements

The authors gratefully acknowledge the NASA Office for Microgravity Materials Science for financial support (Grant No. NAG8-1461).

References

1. D. KLEMPNER and K. C. FRISCH (eds.), "Handbook of Polymeric Foams and Foam Technology" (Hanser, Munich, 1991).
2. K. C. FRISCH and J. H. SAUNDERS (eds.), "Plastic Foams" (Marcel Dekker, NY, 1972).
3. K. W. SUH and D. D. WEBB, "Cellular Materials" in Ency. Polym. Sci. Eng., 2nd ed. Vol. 3 (Wiley, 1985).
4. A. J. CASTRO, US Patent no. 4,247,498 (1981).
5. G. T. CANEBA and D. S. SOONG, *Macromolecules* **18** (1985) 2538.
6. J. H. AUBERT and R. L. CLOUGH, *Polymer* **26** (1985) 2047.
7. J. M. WILLIAMS and J. E. MOORE, *ibid.* **28** (1987) 1950.
8. F. J. TSAI and J. M. TORKELSON, *Macromolecules* **23** (1990) 775.
9. J. E. MARTINI-VVEDENSKY, N. P. SUH and F. A. WALDMAN, US Patent no. 4,473,665 (1984).
10. J. S. COLTON and N. P. SUH, US Patent no. 5,160,674 (1992).
11. S. W. CHA, N. P. SUH, D. F. BALDMAN and C. B. PARK, US Patent no. 5,158,986 (1992).
12. D. F. BALDWIN, N. P. SUH, C. B. PARK and S. W. CHA, US Patent no. 5,334,356 (1996).
13. S. K. GOEL and E. J. BECKMAN, *Polym. Eng. Sci.* **14** (1994) 1137; *ibid.* **14** (1994) 1148.
14. R. APFEL, US Patent no. 5,384,203 (1995).
15. N. QIU and R. APFEL, *Rev. Sci. Instrum.* **66** (1995) 3337.
16. *Idem., J. Mat. Res.* **11** (1996) 2916.
17. K. H. ILLER, *Colloid Polym. Sci.* **258** (1984) 117.
18. I. H. HALL and M. G. PASS, *Polymer* **17** (1976) 807.
19. N. YOSHIHARA, A. FUKUSHIMA, Y. WATANABE, A. NAKAI, S. NOMURA and H. KAWAI, *Sen-i Gakkaishi* **37** (1981) T-387.
20. J. L. WHITE and J. E. SPRUIELL, *Polym. Eng. Sci.* **20** (1980) 247.
21. H. BLADES and J. R. WHITE, US Patent no. 3,227,664 (1966); US Patent no. 3,542,715, (1970).
22. W. H. F. BORMAN, *J. Appl. Polym. Sci.* **22** (1978) 2119.
23. W. H. BONNER, F. H. FISHER and M. Q. WEBB, *ibid.* **24** (1979) 89.
24. J. C. EAST and A. M. GIRSHAB, *Polymer* **23** (1982) 323.
25. O. OLABISI, L. M. ROBESON and M. T. SHAW, "Polymer-Polymer Miscibility" (Academic Press, NY, 1979).
26. M. GILBERT and F. J. HYBART, *Polymer* **13** (1972) 327; *ibid.* **15** (1974) 407.
27. R. S. STEIN and A. MISRA, *J. Polym. Sci.* **18** (1980) 327.
28. M. E. NICHOLS and R. E. ROBERTSON, *J. Polym. Sci., Polym. Phys.* **32** (1994) 573.
29. J. H. HAN and C. D. HAN, *J. Polym. Sci., Polym. Phy. Ed.* **28** (1990) 711; *ibid.* **28** (1990) 743.
30. A. K. LELE and A. D. SHINE, *AIChE J.* **38** (1992), 742; *Idem. Ind. Eng. Chem. Res.* **33** (1994) 1476.
31. D. W. MATSON, J. L. FULTON, R. C. PETERSEN and R. D. SMITH, *ibid.* **26** (1987) 2298.
32. R. C. PETERSON, D. W. MATSON and R. D. SMITH, *Polym. Eng. Sci.* **27** (1987) 1693.
33. P. MISHRA and B. L. DEOPURA, *Rheol. Acta* **23** (1984) 189.
34. K. C. KHEMANI, in ASC Symp. Ser., 1996, 55.

35. F. M. LU and J. E. SPRUIELL, *J. Appl. Polym. Sci.* **33** (1986) 1595.
36. J. ROEBUCK, R. JAKEWAYS and I. M. WARD, *Polymer* **33** (1992) 227.
37. K. SONG and J. L. WHITE, *Polym. Eng. Sci.* **38** (1998) 505.
38. S. Z. D. CHENG, R. PAN, B. WUNDERLICH, *Makromol. Chem.* **189** (1989) 2443.
39. Y. ONISHI and T. NAKAI, *Polym. J.* **24** (1992) 833.
40. M. YAMATO, T. KIMURA and E. ITO, *Kobunshi Ronbunshu* **52** (1995) 110.
41. N. AVRAMOVA, *Polymer* **36** (1995) 801.
42. S. Y. HOBBS and C. F. PRATT, *ibid.* **16** (1975) 462.
43. J. T. YEH and J. RUNT, *J. Polym. Sci. Polym. Phys. Ed.* **27** (1989) 1543.
44. M. E. NICHOLS and R. E. ROBERTSON, *J. Appl. Polym. Sci.* **30** (1992) 755.
45. J. KIM, M. E. NICHOLS and R. E. ROBERTSON, *ibid.* **32** (1994) 887.
46. I. A. AL-RAHEIL and A. M. A. QUDAH, *Polym. Int.* **37** (1995) 47.
47. H. J. LUDWIG and P. EYERER, *Polym. Eng. Sci.* **28** (1988) 143.
48. L. J. GIBSON and M. F. ASHBY, "Cellular Solids," 2nd ed (Univ. Press, Cambridge, 1997).
49. P. H. GEIL, "Polymer Single Crystals" (Wiley, NY, 1963).
50. L. ENGEL, H. KLINGELE, G. W. EHRENSTEIN and H. SCHAPTER, "An Atlas of Polymer Damage" (Prentice Hall, NJ, 1981).
51. A. E. WOODWARD, "Atlas of Polymer Morphology" (Hanser, Munich, 1988).
52. C. A. GARBER and P. H. GEIL, *J. Appl. Phys.* **37** (1966) 4034.
53. G. L. WILKES and C. M. CHU, *J. Appl. Polym. Sci.* **18** (1974) 2221.
54. P. SMITH and A. J. PENNINGS, *J. Polym. Sci., Polym. Phys.* **15** (1977) 523.
55. E. CHANG and S. SLAGOWSKI, *J. Appl. Polym. Sci.* **22** (1978) 769.
56. P. J. BARHAM, M. J. HILL and A. KELLER, *Colloid Polym. Sci.* **258** (1980) 899.
57. P. SMITH, P. J. LEMSTRA, J. P. PIJPERS and A. M. KIEL, *ibid.* **259** (1981) 1070.
58. P. SCHAAF, B. LOTZ and J. C. WITTMAN, *Polymer* **28** (1987) 193.
59. Unpublished results.
60. Z. W. WILCHINSKY, *J. Appl. Phys.* **31** (1960) 1969; *Idem., Adv. X-ray Anal.* **6** (1963) 231.

Received 19 August 1997
and accepted 27 April 1999